LETTER

doi:10.1038/nature09728

The novel gene *twenty-four* defines a critical translational step in the *Drosophila* clock

Chunghun Lim[1]*, Jongbin Lee[2]*, Changtaek Choi[2], Valerie L. Kilman[1], Juwon Kim[2], Sung Mi Park[3], Sung Key Jang[3], Ravi Allada[1] & Joonho Choe[2]

Daily oscillations of gene expression underlie circadian behaviours in multicellular organisms[1]. While attention has been focused on transcriptional and post-translational mechanisms[1–3], other post-transcriptional modes have been less clearly delineated. Here we report mutants of a novel *Drosophila* gene *twenty-four* (*tyf*) that show weak behavioural rhythms. Weak rhythms are accompanied by marked reductions in the levels of the clock protein Period (PER) as well as more modest effects on Timeless (TIM). Nonetheless, PER induction in pacemaker neurons can rescue *tyf* mutant rhythms. TYF associates with a 5′-cap-binding complex, poly(A)-binding protein (PABP), as well as *per* and *tim* transcripts. Furthermore, TYF activates reporter expression when tethered to reporter messenger RNA even *in vitro*. Taken together, these data indicate that TYF potently activates PER translation in pacemaker neurons to sustain robust rhythms, revealing a new and important role for translational control in the *Drosophila* circadian clock.

Transcriptional feedback loops are critical for setting the time of eukaryotic circadian clocks. In *Drosophila*, the *Clock* (*Clk*)/*cycle* (*cyc*) dimer activates the transcription of *period* (*per*), *timeless* (*tim*), *vrille* (*vri*), *PAR domain protein 1* (*Pdp1*) and *clockwork orange* (*cwo*) genes, which in turn feedback to inhibit CLK-activated transcription or regulate *Clk* transcription[2]. These components are also modified post-translationally to alter core clock timing[2,3]. Regulation at multiple levels is thought to impose temporal delays in feedback, allowing sustained oscillations on a circadian time scale.

To discover novel clock components, we performed a genome-wide behavioural screen. Using the Korea Advanced Institute of Science and Technology (KAIST) GenExel *Drosophila* library, we identified ~4,000 EP lines containing P elements bearing the upstream activating sequence (UAS) for the yeast Gal4 transcription factor inserted near transcription start sites. These flies were crossed with transgenic flies expressing *GAL4* under the control of the *tim* promoter (*tim-GAL4*) to drive downstream gene expression in clock cells[4]. One EP line identified by a long-period rhythm was the G10872 line that contains an insertion 893 bp upstream of the *CG4857* transcription start site (Supplementary Fig. 1a). Sequence analyses of the predicted amino acid sequence for *CG4857* did not reveal any apparent functional domains or obvious vertebrate homologues but did reveal conservation with genes from different *Drosophila* species and other insects (Supplementary Fig. 2). We termed this novel gene *twenty-four* (*tyf*).

To characterize the phenotype in flies bearing *tyf* loss-of-function mutations, we generated a ~2.5 kb deletion by imprecise P-element excision (Supplementary Fig. 1a; $tyf^{\Delta G14151}$; tyf^{1}), deleting amino acids 79–449 of *tyf* and resulting in a frame-shift and premature termination. In addition, we identified a *piggyBac* insertion line that shows markedly reduced levels of *tyf* transcript (tyf^{e00614}; tyf^{e}) without affecting the transcript levels of adjacent genes (Supplementary Fig. 1b). Wild-type *Drosophila* show morning and evening peaks under 12 h light:12 h dark cycles, anticipate the transitions between light-on and light-off by gradually increasing their activity, and maintain their locomotor rhythm in subsequent constant dark. In *tyf* mutants, morning anticipation of lights-on was reduced and their rhythm was immediately less robust, resulting in weak but long periods in constant dark (Fig. 1 and Supplementary Table 1). Precise *piggyBac* excision in tyf^{e} restored wild-type circadian behaviour (Supplementary Table 1), indicating that *tyf* gene disruption is responsible for its circadian phenotype. Analyses in trans-heterozygous females show that *tyf* alleles are recessive and not complemented by deletions of the *CG4857* locus (Supplementary Fig. 3).

Although circadian clocks are evident in multiple tissues, brain clocks are largely responsible for circadian behaviours[4]. Neuroanatomical studies have established two oscillator models in which distinct groups of clock cells control morning and evening locomotor activity and behavioural rhythms[5,6]. The neuropeptide gene *Pigment-dispersing factor* (*Pdf*), expressed in ventral lateral neurons (LNs), has been implicated in driving morning anticipation and resetting evening clocks in the dorsal LNs/dorsal neurons (DNs)[7–9]. To map the neurons important for *tyf* effects, we generated *tyf-GAL4* lines containing the *tyf* promoter region (from −3.0 kb to +0.5 kb), and visualized its expression using a UAS–GFP reporter. *tyf-GAL4* expression was relatively restricted to a subset of neurons in the adult brain (Supplementary Fig. 4a–f). Anti-PER antibody staining revealed that it is strongly expressed in PDF^{+} ventral LNs and weakly in dorsal LNs assessed in independent lines (data not shown). In contrast, *tyf-GAL4* expression was not detectable in the DNs. Consistent with the idea that *tyf-GAL4* reflects endogenous *tyf* expression, *tyf-GAL4* along with a UAS-*tyf* transgene fully rescues the behavioural phenotypes in *tyf* mutants (data not shown).

To map the loci of *tyf* function, we restricted TYF overexpression to the PDF^{+} ventral LNs using *Pdf-GAL4* (ref. 7). This results in a long period, similar to with the *tim-GAL4* driver, whereas Gal4 inhibition in PDF^{+} cells by a *Pdf-GAL80* transgene[5] suppressed the long period phenotype (Supplementary Table 2). Independent UAS-*tyf* insertions confirmed these results. TYF expression restricted to PDF^{+} cells was also sufficient to rescue free-running locomotor rhythms in mutants (Supplementary Table 3). In addition, RNA interference (RNAi)-mediated knockdown of *tyf* expression in PDF^{+} cells phenocopied circadian behaviours in *tyf* hypomorphic mutants (Supplementary Table 3). These data indicate that *tyf* expression in the PDF^{+} pacemaker neurons is necessary and sufficient for robust behavioural rhythms.

To determine *tyf* effects on the core clock, we analysed molecular rhythms from head extracts, which largely reflect eye clocks[10]. We found that cycling expression of PER, TIM and PDP1 proteins in *tyf* mutants is comparable to wild type (data not shown). *tyf* transcript levels were relatively constant in a light–dark cycle and not affected in clock mutants (Supplementary Fig. 4g, h). We then focused on the behaviourally relevant pacemaker neurons. Anti-PDF immunofluorescence revealed

[1]Department of Neurobiology and Physiology, Northwestern University, Evanston, Illinois 60208, USA. [2]Department of Biological Sciences, Korea Advanced Institute of Science and Technology, Daejeon 305-701, Korea. [3]Department of Life Sciences, Pohang University of Science and Technology, Pohang 790-784, Korea.
*These authors contributed equally to this work

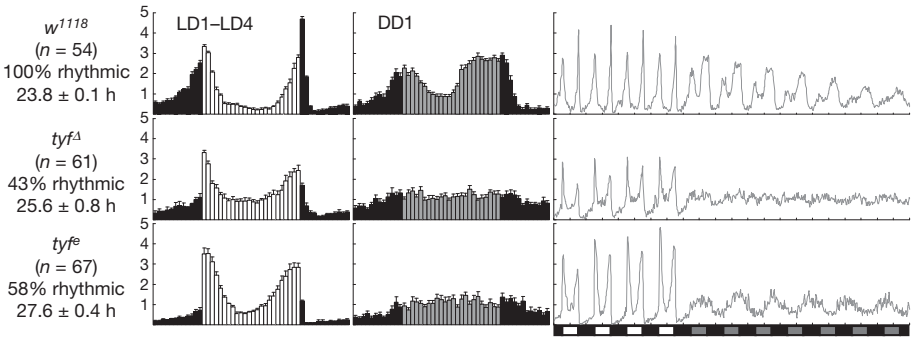

Figure 1 | Robust behavioural rhythms require *tyf*. Averaged activity profiles during 4 light–dark (LD1–LD4)/first constant dark (DD1) cycles (middle panel) and actograms throughout the behavioural analyses (right panel) ($n = 54–67$). Percentage of rhythmic flies and period ± s.e.m. ($n = 26–54$) under constant dark cycles are given at the left. Error bars indicate s.e.m. White/black bars, light–dark cycle; grey/black bars, constant dark cycle.

no overt defects in the neural projections from PDF$^+$ ventral LNs of *tyf* mutants (Supplementary Fig. 5a). Adult-specific TYF expression using a drug-inducible Gal4 was sufficient for behavioural rescue in *tyf* mutants (Supplementary Table 4 and Supplementary Fig. 5c), further reducing the likelihood that *tyf* phenotypes are due to developmental defects.

Notably, we found that PER protein was barely detectable in LN clock cells of *tyf* mutants (Fig. 2a). PER cycling was dampened but not absent (Fig. 2b and Supplementary Fig. 6). *tyf* mutant effects were less severe in the DNs with PER at ~50% of wild-type peak levels. TYF expression in PDF$^+$ neurons rescued PER cycling only in PDF$^+$ clock cells of *tyf* mutants (Supplementary Fig. 7). Consistent with marked PER reductions, PDF levels increased in dorsal projections from the small ventral LNs of *tyf* mutants (Supplementary Fig. 5b), as observed in *per*^{01} flies[11]. TIM levels were also reduced in *tyf* mutants, but to a lesser extent than PER, with peak levels in *tyf* mutants reduced to ~50% of wild type (Supplementary Fig. 8a). Such effects may be indirect through PER, as we found that TIM reductions were also observed in *per*^{01} flies and there was little effect of loss of *tyf* on TIM in *per*^{01} mutants.

In contrast to strong effects on PER, *tyf* mutants normally expressed PDP1ε, CWO and CLK proteins (Fig. 2a and Supplementary Fig. 8b). The oscillating expression of PDP1ε protein as well as *tim* and *Pdp1ε* transcripts in *tyf* mutants was comparable to wild type (Supplementary Fig. 8c, d). We reason that light–dark cycles, the clock neural network and/or multiple feedback loops may buffer the molecular clock against loss of *tyf* function.

Given that the robust reductions in PER may be responsible for the arrhythmic behaviour, we proposed that PER expression via the *GAL4*/UAS system could rescue *tyf* locomotor rhythms[12]. Indeed, we find that PER, but not TIM or CLK, overexpression specifically in PDF$^+$ cells of *tyf* mutants restored wild-type levels of rhythmicity (Fig. 3, Supplementary Fig. 9 and Supplementary Table 5). These rescue data indicate that neither post-translational regulation of PER protein by TIM[3] nor transcriptional activation of *per* gene expression by CLK[2] would be limiting for normal circadian behaviour in *tyf* mutants. Moreover, these behavioural data indicate that PER is a major target of TYF in PDF neurons.

We next examined at what regulatory step PER expression in *tyf* mutants is compromised. We observed that PER protein, but not *per* RNA levels were reduced in brain extracts (data not shown). Although consistent with post-transcriptional regulation, we cannot exclude the possibility that this result could arise from the masking effect of low-level non-cycling *per* RNA in non-circadian tissues. *tyf* effects were not evident on a CLK-activated *per* promoter-*GAL4* transgene (Supplementary Fig. 10) but were evident on a *per* transgene lacking its

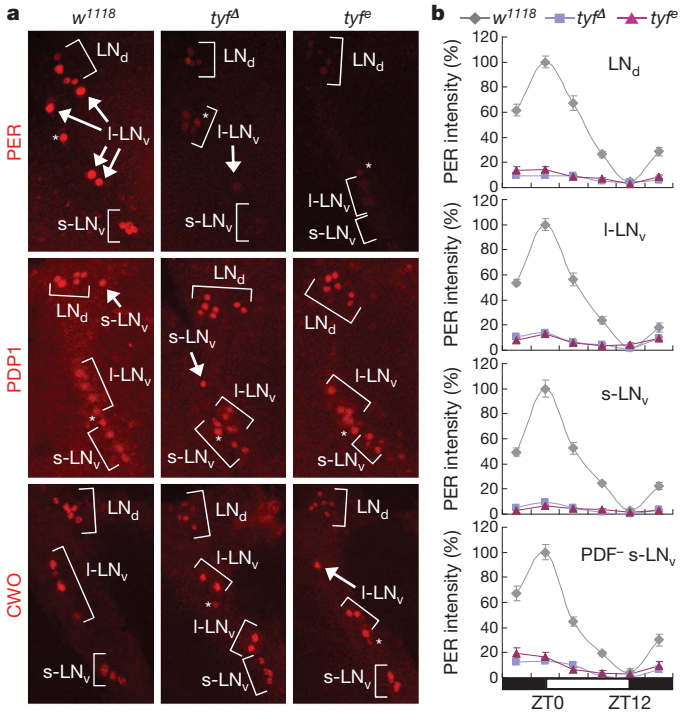

Figure 2 | *tyf* is crucial for PER expression in pacemaker neurons. a, Adult brains were immunostained with anti-PER (top, ZT0), anti-PDP1 (middle, ZT21) and anti-CWO (bottom, ZT3) antibodies. Clock cell groups were imaged with a ×60 oil objective lens and identified by co-staining with anti-PDF antibody (data not shown). LN_d, dorsal lateral neuron; l-LN_v, large ventral LN; s-LN_v, small ventral LN. Asterisk indicates PDF-negative small ventral LN. **b**, PER intensity in each clock cell group was quantified, averaged ($n = 7–10$), and normalized to the value of wild-type *Drosophila* at ZT0, which was set as 100%. Error bars indicate s.e.m.

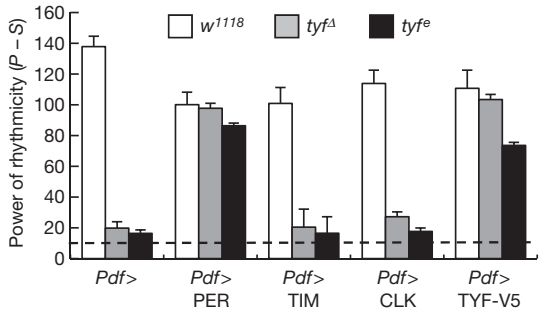

Figure 3 | PER induction rescues *tyf* mutant rhythms. Each clock gene was overexpressed in PDF$^+$ cells of wild-type or *tyf* mutants and their rhythmicity under constant dark cycles was measured by power (P) − significance (S) values. *x*-axis shows *Pdf-GAL4*-driven overexpression of each clock transgene. Of note, each fly with $P - S$ values greater than 10 (dotted line) is defined as rhythmic. Data represent average + s.e.m. ($n = 18–48$).

natural promoter[13] (Supplementary Fig. 11a), indicating that the *per* promoter is not necessary nor sufficient for *tyf* effects. *tyf* effects were also still observed on a *per*(Δ)-HA-His transgene that lacks the Doubletime (DBT)-binding domain, thus reducing DBT-mediated PER degradation[14]. We then examined PER in *Drosophila* in which we rescued *tyf* by PER overexpression. Interestingly, neither PER levels driven by constitutive *Pdf-GAL4* nor oscillations were affected in *tyf* mutants (Supplementary Fig. 11b), indicating that *tyf* is not required for post-translational regulation of PER. The lack of most *per* 5′ and 3′ untranslated regions (UTRs) in the UAS-*per* transgene[15] and/or *per* overexpression itself may compensate for loss of *tyf*. Taken together, our observations indicate that *tyf* post-transcriptionally regulates *per* expression.

We next asked whether TYF associates with post-transcriptional regulatory factors, circadian clock components and/or specific RNA targets using immunoprecipitation of carboxy-terminally V5-tagged TYF (TYF–V5). We confirmed that *GAL4*/UAS-driven TYF–V5 rescues behavioural rhythms in *tyf* mutants (Fig. 3 and Supplementary Table 5) and that TYF–V5 expression is cytoplasmic at all times of day (Supplementary Fig. 4i). TYF–V5 driven by *tim-GAL4* was immunoprecipitated from head extracts and then TYF-associating proteins were probed with different antibodies. TYF did not associate with either PER or TIM (Fig. 4a). However, poly(A)-binding protein (PABP) was specifically co-immunoprecipitated with TYF at two times of the day in an RNase-insensitive manner (Fig. 4a, data not shown). *In vitro* assays demonstrated that PABP interacts with the amino-terminal region of TYF (Supplementary Fig. 12a; TYF-N, amino acids 1–1167).

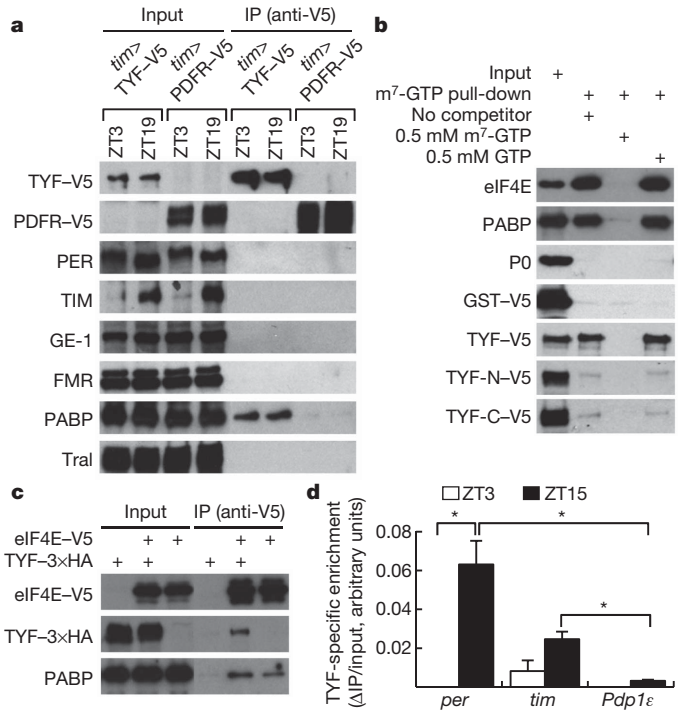

Figure 4 | TYF specifically associates with the 5′-cap-binding complex PABP, and target gene transcripts. **a**, *Drosophila* head extracts were immunoprecipitated (IP) with anti-V5 antibody. Bound proteins were probed with antibodies shown on the left. **b**, **c**, S2 cell extracts expressing epitope-tagged TYF were incubated with m^7-GTP sepharose beads (**b**) or immunoprecipitated with anti-V5 agarose beads (**c**). Where indicated, 0.5 mM of soluble competitor was added to the extracts. Bound proteins were detected similarly as in **a**. Input, 3% of extract included in each binding assay. **d**, After the immunoprecipitation of TYF-V5 from *Drosophila* head extracts, bound RNAs were quantitatively analysed by real-time RT–PCR ($n = 2$, in triplicates). TYF-specific fold enrichment was calculated by normalizing RNA levels in TYF immunoprecipitates to input levels and then subtracting the normalized value of control immunoprecipitation (PDFR–V5). Error bars indicate s.e.m. *$P < 0.05$ as determined by Student's *t*-test.

It has been proposed that PABP stimulates translation in part by binding to both 5′- cap-associating translation initiation factor eIF4G and the poly(A) tail in mRNAs, thereby facilitating mRNA circularization[16]. Therefore, we also examined a possible association of TYF with a cap-binding complex using 5′-cap (7-methylguanosine, m^7-GTP) affinity beads and S2 cell extracts expressing epitope-tagged TYF. We found that eIF4E, a translation initiation factor directly recognizing the 5′-cap structure, PABP and TYF were efficiently and specifically pulled-down by m^7-GTP affinity beads in an RNase-insensitive manner (Fig. 4b and Supplementary Fig. 12b). Addition of soluble m^7-GTP but not GTP inhibited their cap association, validating the specificity. Interestingly, the N-terminal portion of TYF, capable of *in vitro* PABP binding (Supplementary Fig. 12a), shows strongly reduced affinity for the 5′ cap, indicating that PABP may not solely mediate TYF association with the 5′ cap. Our results link TYF to RNA-binding proteins involved in translation.

We checked further whether TYF associates with clock gene transcripts. RNA in TYF–V5 immunoprecipitates was analysed by real-time reverse transcriptase polymerase chain reaction (RT–PCR) (Fig. 4d). To quantify TYF-specific transcript enrichment, we normalized RNA levels in TYF immunoprecipitates to input RNA and then subtracted the signal from a background control immunoprecipitation (PDFR–V5) also normalized to input. We find that TYF pulls-down significant amounts of *per* and *tim* RNAs relative to the amounts of *Pdp1* at the times of their peak expression levels (Zeitgeber time (ZT)15, $P < 0.029$). Moreover, *per* RNA levels in TYF immunoprecipitates were higher at their peak times than trough times (that is, ZT15 versus ZT3) even after normalizing for input levels ($P < 0.026$). As *Pdp1* has comparable input levels to *per* and *tim* (data not shown), the low *Pdp1* signal is unlikely to be explained by low input levels. However, differential anatomical distributions could contribute to these results[17]. We also did not detect significant TYF-specific signal for *Clk* and *cyc* RNAs in immunoprecipitated RNA, although low input levels could explain the lack of detectable association (data not shown). We could not identify any RNA-recognition motifs in TYF, indicating that RNA-binding intermediaries, such as eIF4E and PABP, may mediate its association with RNA.

To address whether TYF is incorporated into translating ribonucleocomplexes, we fractionated S2 cell extracts expressing TYF–3×HA by sucrose density gradient in the absence or presence of EDTA to dissociate ribosomes (Supplementary Fig. 13). Sedimentation profiles demonstrated that ribosomal proteins P0 and PABP were present in polysomal fractions in an EDTA-sensitive manner. In contrast, a minor fraction of TYF co-sedimented with polysomes and showed a modest shift with EDTA. This pattern is similar to that of eIF4E, consistent with their association (Fig. 4b, c). Taken together, the association of TYF with eIF4E, PABP and *per* RNA indicates a direct role in PER protein synthesis, possibly at a translation initiation step.

To investigate the effects of *tyf* on its associating RNAs, we performed an RNA-tethering assay in cultured S2 cells[18]. TYF fused to the RNA-binding bacteriophage MS2 coat protein is tethered to a luciferase reporter RNA containing MS2-binding sites (Fig. 5a). TYF activity is monitored by assaying luciferase activity. TYF–MS2, compared to MS2 alone, enhanced luciferase expression in an MS2-binding-site-dependent manner (Fig. 5b). The C-terminal region of TYF (TYF-C, amino acids 1161–1911) was necessary and sufficient for the activation (Fig. 5b and Supplementary Fig. 14a–c). TYF–MS2 activation was augmented if the *per* or *tim* 3′ UTR was fused to the reporter gene but not the *cyc* 3′ UTR (Fig. 5b and Supplementary Fig. 14d). TYF without the MS2 domain could not activate reporter containing both *per* 5′ and 3′ UTRs, consistent with a requirement for other RNA-binding proteins (Supplementary Fig. 14h). Notably, we found that a transgenic fusion between the *per* coding region and luciferase lacking the *per* 3′ UTR (XLG-luc)[19] was also reduced in *tyf* mutants, indicating that the *per* 3′ UTR is not necessary for *tyf* effects *in vivo* (data not shown). In contrast to reporter activity, reporter RNA levels and

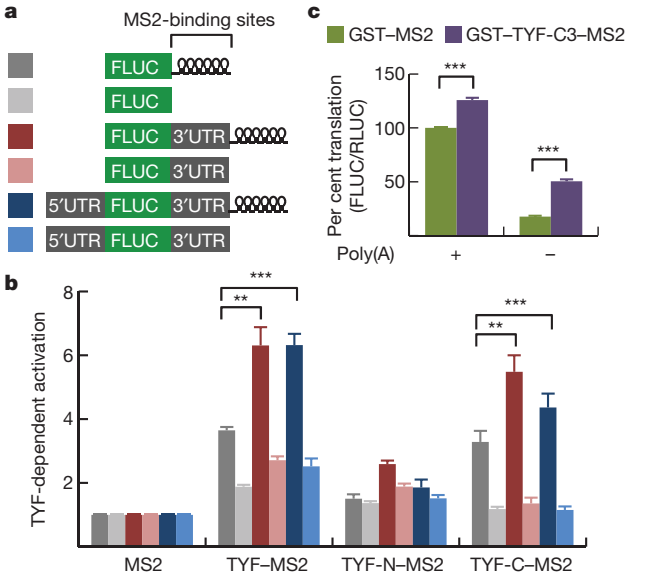

Figure 5 | TYF activates reporter expression when tethered to its RNA. **a**, **b**, S2 cells were transfected with MS2 reporter plasmid (depicted in **a**) and expression vector for MS2 fusion protein. Firefly luciferase activity (FLUC) was first normalized to *Renilla* luciferase activity (RLUC). Fold increase in activation was then calculated by normalizing to the value in the presence of MS2. Data represent average + s.d. ($n = 4$–6). 5′ UTR and 3′ UTR are in *per*. $^{**}P < 0.01$ and $^{***}P < 0.001$ as determined by Student's *t*-test. **c**, m^7-G-capped MS2 reporter RNAs were synthesized using *in vitro* transcription, polyadenylated by bacterial poly(A) polymerase, and incubated with translation-competent S2 cell extracts and purified GST–MS2 fusion protein in *in vitro* translation reactions. Luciferase assays were performed as in **b**. Data represent average + s.e.m. ($n = 3$–7). $^{***}P < 0.001$ as determined by one-way ANOVA, Tukey post-hoc test.

nuclear/cytoplasmic distribution were comparable between MS2- and TYF–MS2-transfected cells (Supplementary Fig. 14e, f). Moreover, analytical centrifugation through a sucrose cushion revealed that more reporter transcripts associate with high-density ribosomes in the presence of TYF–MS2 (Supplementary Fig. 14g; $P < 0.027$), further supporting a role in translational control.

To more directly test the translational activation function of TYF, we reconstituted this tethering system in *in vitro* translation assays. A C-terminal TYF region (TYF-C3, amino acids 1373–1911) fused to MS2, which robustly activated MS2 reporter expression in transfected cells (data not shown), was bacterially expressed, purified and incubated with *in vitro* transcribed MS2 reporter RNAs and translation-competent S2 cell extracts. TYF-C3–MS2 activated translation from a m^7-G capped and poly(A)-tailed reporter RNA modestly (Fig. 5c; $P < 0.001$) and a non-polyadenylated RNA more strongly (2.9×, $P < 0.001$). TYF-C3–MS2 effects are evident without affecting reporter RNA levels (data not shown). Moreover, this TYF region is not sufficient to bind PABP *in vitro* (Supplementary Fig. 12a), indicating that these effects are not mediated by PABP recruitment. These data clearly demonstrate a translation activation function of TYF *in vitro*, supporting a possible role in translation of poorly adenylated transcripts.

Relative to studies of transcriptional and post-translational regulation, little is known about other post-transcriptional/translational mechanisms of core clock regulation in different organisms[3,20]. Although a number of RNA-binding proteins are either rhythmically expressed[1] or important for behavioural rhythms[21–24], direct links between specific trans-acting factors, specific clock gene transcripts, and *in vivo* core clock function have yet to be clearly established, especially in metazoans. Indeed, a number of studies have indicated a role for post-transcriptional regulation in modulating *per* expression[10,25–28]. Here we demonstrate with several lines of evidence that TYF activates PER translation to sustain behavioural rhythms, revealing a new and important role for translational control in the *Drosophila* circadian clock. We observe robust *tyf* effects on PER and lesser effects on TIM yet no detectable reduction of the other core clock components we assayed. This observation indicates that impairing *tyf*-dependent translation is not critical for the expression of most clock components. Importantly, transgenic induction of PER, but not other clock components including TIM, can rescue *tyf* mutant phenotypes.

TYF function is especially important in pacemaker neurons. Both *tyf* and *per* expression in PDF^+ ventral LNs is sufficient to strongly rescue behavioural rhythms in *tyf* mutants. Moreover, *tyf* effects on PER are, by far, most evident in these pacemaker neurons. The brain pacemaker neurons are also among the few clock cells that demonstrate robust free-running molecular rhythms in constant dark[8,9]. Thus, TYF-mediated translational control may be a specialization of networked pacemakers in the brain crucial for sustaining free-running rhythmicity.

Our data also strongly support the model that TYF acts at the level of translational control. TYF associates with *per* and *tim* RNAs, as well as translational regulatory components such as the eIF4E-containing 5′-cap-binding complex and PABP, of which the latter is insensitive to RNase treatment. In addition, TYF tethered to a reporter RNA via MS2 can activate reporter expression without altering RNA levels in transfected cells and, importantly, in cell extracts providing exogenous RNA templates and purified TYF–MS2.

It remains unclear how TYF controls translation of its target RNAs. We observe specific effects on PER and TIM but not on other clock components, and we find that TYF interacts with translation components such as the eIF4E-containing cap-binding complex and PABP. We propose that RNA-binding translational repressors associate with newly transcribed *per* RNA, temporarily postpone translation and thus delay PER feedback repression on its own transcription (Supplementary Fig. 15). Such a delay could contribute to the observed lag between protein and RNA particularly in pacemaker neurons, although post-translational mechanisms may also contribute, at least in the eyes[29]. TYF, which does not have a known RNA-recognition motif, could then be recruited to target transcripts by these translational repressors, releasing them to stimulate initiation of *per* translation. We have not been able to biochemically or genetically link TYF to RNA-binding proteins FMR, LARK, or the translation regulator *Thor*/4E-BP, which have been shown to contribute to circadian clock function[21,22,24]. Nonetheless, TYF association with eIF4E and their similar polysome profiles implicate TYF as a novel translation initiation factor. In addition, the effects of TYF may be more evident on poorly adenylated transcripts on the basis of our *in vitro* data (Fig. 5c). Of note, the *Drosophila* homologue of the clock-regulated deadenylase *nocturnin*[30] has been shown to be important in DNs for circadian light responses but neither a LN function nor an RNA target has been described[24]. Nevertheless, unique features of TYF-regulated transcripts may mediate the highly selective TYF effects on clock components *in vivo*.

Post-transcriptional regulation on *per* RNA has been considered to be modulatory to clock function. The identification of a critical role for TYF highlights an important role for PER translation in the *Drosophila* neural clockwork. It will be of interest to determine if proteins functionally analogous to TYF serve similarly important and specific functions in the mammalian clock.

METHODS SUMMARY

Plasmids. Total RNA from adult *Drosophila* heads was isolated using Trizol reagent and reverse-transcribed using Superscript III according to the manufacturer's instructions (Invitrogen). *tyf* complementary DNA (cDNA) was PCR-amplified by Platinum *Pfx* polymerase (Invitrogen) with the appropriate primer sets and inserted into pUAST vector for regular germline transformation and into its modified version with *attB* site and C-terminal V5 tag for site-specific germline transformation.

***Drosophila* stocks.** All flies were reared with standard cornmeal-yeast-agar medium at 25 °C under light–dark (12 h light:12 h dark) cycles. EP lines G10872 and G14151 were obtained from the KAIST GenExel *Drosophila* library. To generate a *tyf* deletion line ($tyf^{\Delta 1}$), P-element excision lines were established from the G14151 line and molecularly characterized by genomic DNA-PCR with the appropriate primer sets. *Df(1)HC244*, *Df(1)rb23* and UAS-mCD8–GFP lines were obtained from the Bloomington *Drosophila* stock centre. The UAS-tyf^{RNAi} line was obtained from the National Institute of Genetics (Japan). Several independent germline transformants were established from w^{1118} embryos injected with UAS-*tyf* transgenic construct (BestGene).

Full Methods and any associated references are available in the online version of the paper at www.nature.com/nature.

Received 16 April 2009; accepted 1 December 2010.

1. Doherty, C. J. & Kay, S. A. Circadian control of global gene expression patterns. *Annu. Rev. Genet.* **44,** 419–444 (2010).
2. Zheng, X. & Sehgal, A. Probing the relative importance of molecular oscillations in the circadian clock. *Genetics* **178,** 1147–1155 (2008).
3. Harms, E., Kivimae, S., Young, M. W. & Saez, L. Posttranscriptional and posttranslational regulation of clock genes. *J. Biol. Rhythms* **19,** 361–373 (2004).
4. Dubruille, R. & Emery, P. A plastic clock: how circadian rhythms respond to environmental cues in *Drosophila*. *Mol. Neurobiol.* **38,** 129–145 (2008).
5. Stoleru, D., Peng, Y., Agosto, J. & Rosbash, M. Coupled oscillators control morning and evening locomotor behaviour of *Drosophila*. *Nature* **431,** 862–868 (2004).
6. Grima, B., Chelot, E., Xia, R. & Rouyer, F. Morning and evening peaks of activity rely on different clock neurons of the *Drosophila* brain. *Nature* **431,** 869–873 (2004).
7. Renn, S. C., Park, J. H., Rosbash, M., Hall, J. C. & Taghert, P. H. A *pdf* neuropeptide gene mutation and ablation of PDF neurons each cause severe abnormalities of behavioral circadian rhythms in *Drosophila*. *Cell* **99,** 791–802 (1999).
8. Peng, Y., Stoleru, D., Levine, J. D., Hall, J. C. & Rosbash, M. *Drosophila* free-running rhythms require intercellular communication. *PLoS Biol.* **1,** e13 (2003).
9. Lin, Y., Stormo, G. D. & Taghert, P. H. The neuropeptide pigment-dispersing factor coordinates pacemaker interactions in the *Drosophila* circadian system. *J. Neurosci.* **24,** 7951–7957 (2004).
10. Zeng, H., Hardin, P. E. & Rosbash, M. Constitutive overexpression of the *Drosophila* period protein inhibits period mRNA cycling. *EMBO J.* **13,** 3590–3598 (1994).
11. Park, J. H. *et al.* Differential regulation of circadian pacemaker output by separate clock genes in *Drosophila*. *Proc. Natl Acad. Sci. USA* **97,** 3608–3613 (2000).
12. Yang, Z. & Sehgal, A. Role of molecular oscillations in generating behavioral rhythms in *Drosophila*. *Neuron* **29,** 453–467 (2001).
13. Frisch, B., Hardin, P. E., Hamblen-Coyle, M. J., Rosbash, M. & Hall, J. C. A promoterless period gene mediates behavioral rhythmicity and cyclical per expression in a restricted subset of the *Drosophila* nervous system. *Neuron* **12,** 555–570 (1994).
14. Kim, E. Y., Ko, H. W., Yu, W., Hardin, P. E. & Edery, I. A. DOUBLETIME kinase binding domain on the *Drosophila* PERIOD protein is essential for its hyperphosphorylation, transcriptional repression, and circadian clock function. *Mol. Cell. Biol.* **27,** 5014–5028 (2007).
15. Blanchardon, E. *et al.* Defining the role of *Drosophila* lateral neurons in the control of circadian rhythms in motor activity and eclosion by targeted genetic ablation and PERIOD protein overexpression. *Eur. J. Neurosci.* **13,** 871–888 (2001).
16. Sonenberg, N. & Hinnebusch, A. G. Regulation of translation initiation in eukaryotes: mechanisms and biological targets. *Cell* **136,** 731–745 (2009).
17. Kula-Eversole, E. *et al.* Surprising gene expression patterns within and between PDF-containing circadian neurons in *Drosophila*. *Proc. Natl Acad. Sci. USA* **107,** 13497–13502 (2010).
18. Keryer-Bibens, C., Barreau, C. & Osborne, H. B. Tethering of proteins to RNAs by bacteriophage proteins. *Biol. Cell* **100,** 125–138 (2008).
19. Veleri, S., Brandes, C., Helfrich-Forster, C., Hall, J. C. & Stanewsky, R. A self-sustaining, light-entrainable circadian oscillator in the *Drosophila* brain. *Curr. Biol.* **13,** 1758–1767 (2003).
20. Staiger, D. & Koster, T. Spotlight on post-transcriptional control in the circadian system. *Cell. Mol. Life Sci.* doi:10.1007/s00018–010–0513–5 (in the press).
21. Dockendorff, T. C. *et al.* *Drosophila* lacking *dfmr1* activity show defects in circadian output and fail to maintain courtship interest. *Neuron* **34,** 973–984 (2002).
22. Sofola, O. *et al.* The *Drosophila* FMRP and LARK RNA-binding proteins function together to regulate eye development and circadian behavior. *J. Neurosci.* **28,** 10200–10205 (2008).
23. Kadener, S. *et al.* A role for microRNAs in the *Drosophila* circadian clock. *Genes Dev.* **23,** 2179–2191 (2009).
24. Nagoshi, E. *et al.* Dissecting differential gene expression within the circadian neuronal circuit of *Drosophila*. *Nature Neurosci.* **13,** 60–68 (2010).
25. So, W. V. & Rosbash, M. Post-transcriptional regulation contributes to *Drosophila* clock gene mRNA cycling. *EMBO J.* **16,** 7146–7155 (1997).
26. Stanewsky, R., Jamison, C. F., Plautz, J. D., Kay, S. A. & Hall, J. C. Multiple circadian-regulated elements contribute to cycling period gene expression in *Drosophila*. *EMBO J.* **16,** 5006–5018 (1997).
27. Majercak, J., Sidote, D., Hardin, P. E. & Edery, I. How a circadian clock adapts to seasonal decreases in temperature and day length. *Neuron* **24,** 219–230 (1999).
28. Suri, V., Lanjuin, A. & Rosbash, M. TIMELESS-dependent positive and negative autoregulation in the *Drosophila* circadian clock. *EMBO J.* **18,** 675–686 (1999).
29. Suri, V., Hall, J. C. & Rosbash, M. Two novel doubletime mutants alter circadian properties and eliminate the delay between RNA and protein in *Drosophila*. *J. Neurosci.* **20,** 7547–7555 (2000).
30. Green, C. B. *et al.* Loss of Nocturnin, a circadian deadenylase, confers resistance to hepatic steatosis and diet-induced obesity. *Proc. Natl Acad. Sci. USA* **104,** 9888–9893 (2007).

Supplementary Information is linked to the online version of the paper at www.nature.com/nature.

Acknowledgements We thank I. Edery, J. Hall, H. Keshishian, M. Rosbash, F. Rouyer, A. Sehgal, the Bloomington *Drosophila* stock center, Harvard Exelixis *Drosophila* stock collection, KAIST GenExel *Drosophila* library and the National Institute of Genetics for *Drosophila* strains; P. Hardin, E. Izaurralde, A. Nakamura, M. Rosbash and N. Sonenberg for antibodies; J. Lykke-Andersen for plasmids; K. E. Duncan for suggestions on *in vitro* translation assays. This work was supported by grants from the Brain Research Center of the 21st Century Frontier Research Program through the National Research Foundation of Korea funded by the Ministry of Education, Science and Technology, the Republic of Korea (J.C.) and from the National Institutes of Health (R01NS059042, R01NS052903, R01MH067870; R.A.)

Author Contributions R.A. and J.C. conceived the study; R.A., C.L. and J.C. designed the experiments; C.L. (under the supervision of R.A.) and J.L (under the supervision of J.C.) jointly completed Figs 1 and 2, Supplementary Figs 1, 4, 8, 14 and Supplementary Tables 2 and 3; J.L., S.M.P. and S.K.J. performed and analysed the experiments in Supplementary Fig. 13; J.L., C.C. and J.K. performed the genome-wide behavioural screen; C.C. performed GST pull-down studies in Supplementary Fig. 12a; V.L.K. performed PDF quantification analysis in Supplementary Fig. 5b; C.L. performed and analysed experiments in all remaining Figures, Supplementary Figures and Tables; C.L. and R.A. wrote the manuscript.

Author Information Reprints and permissions information is available at www.nature.com/reprints. The authors declare no competing financial interests. Readers are welcome to comment on the online version of this article at www.nature.com/nature. Correspondence and requests for materials should be addressed to R.A. (r-allada@northwestern.edu) or J.C. (jchoe@kaist.ac.kr).

METHODS

Plasmids. *Pabp* cDNA was amplified and inserted into pGEX-4T-1 (GE Healthcare) to purify GST–PABP protein from bacteria. To make a DNA construct for *tyf-GAL4* transgenic *Drosophila*, the *tyf* gene promoter region ranging from −3.0 kb to +0.5 kb relative to the transcription start site was PCR-amplified from wild-type genomic DNA and inserted into the pPTGAL4 vector[31]. cDNAs encoding an oligomerization-defective MS2 coat protein mutant and six tandem repeats of MS2 coat protein binding site (6×BS) were PCR-amplified from pcNMS2–Flag and pcB6bs[32], respectively, and inserted into pAc5.1/V5 (Invitrogen). Firefly or *Renilla* luciferases cDNA with or without clock gene UTRs was inserted into pAc5.1/V5 or pAc/6×BS to generate MS2 reporter plasmids. cDNAs corresponding to wild type or deletion mutants of *tyf* were inserted into: (1) pAc5.1/V5 or pAc/MS2-V5 to express C-terminal V5 or MS2-V5 fusion proteins in transfected S2 cells; and (2) pcDNA3 (Invitrogen) for *in vitro* transcription and translation.

***Drosophila* stocks and behavioural assays.** *Pdf-GAL4*, *tim-GAL4*, *per-GAL4*, *Elav*-Gene Switch-*GAL4*, *Pdf-GAL80*, *cry-GAL80*, UAS-*per16*, UAS-*tim*, UAS-*Clk*, *perG*, *per*(Δ)-HA-His, XLG-luc, and 7.2:9 transgenic lines were described previously[5,7,10,13–15,19,33–36]. For phiC31 integrase-based transformation[37], the UAS-*tyf*-V5 transgene was inserted into the *attP*40 landing site[38] (Genetic Services). The locomotor activity of individual male or virgin female *Drosophila* was measured using *Drosophila* Activity Monitors (Trikinetics) and analysed using ClockLab analysis software (Actimetrics) as described previously[39]. For adult-specific TYF overexpression, flies were fed with foods containing 0.5 mM RU486 (dissolved in 4% ethanol) or vesicle control (4% ethanol) from the first light–dark cycle of their behavioural assays to activate Gene Switch-*GAL4* (ref. 36) and induce TYF overexpression from UAS-*tyf* transgenes.

Quantitative RT–PCR. Semi-quantitative and real-time RT–PCR using total RNA from adult *Drosophila* heads and transfected S2 cells were performed as described previously[39,40]. Primer sequences used in our transcript analyses are available on request.

Immunostaining. Whole-mount immunostaining in adult *Drosophila* brains was performed as described previously[40]. For primary antibodies, we used rabbit anti-PER (a gift from M. Rosbash), rabbit anti-PDP1[40] and guinea pig anti-TIM[40], guinea pig anti-CWO[41] and anti-CLK[42], mouse anti-PDF (Developmental Studies Hybridoma Bank) and anti-V5 (Invitrogen) antibodies. Anti-mouse IgG Alexa 488, anti-mouse IgG Alexa 594, anti-rabbit IgG Alexa 594, anti-guinea pig IgG Alexa 594 and 633 antibodies (Invitrogen) were used for fluorescence-conjugated secondary antibodies. Images were obtained using confocal laser-scanning microscopes (Nikon C1 or Carl Zeiss Pascal). For the quantitative analysis, signal intensity from each group of clock cells was quantified using ImageJ software as described previously[43].

Immunoprecipitation. Immunoprecipitation from *Drosophila* head and S2 extracts were performed as described previously[40]. For RNA analysis, ~200 *Drosophila* heads were homogenized in a lysis buffer (25 mM Tris-Cl pH 7.5, 300 mM NaCl, 10% glycerol, 1 mM EDTA, 1 mM dithiothreitol, 0.5% Nonidet P-40, 1 mM phenylmethylsulfonyl fluoride) containing 20 U ml^{-1} DNase I (Promega), 100 U ml^{-1} RNasin (Promega) and 8 mM vanadyl ribonucleoside complex (Sigma). After the immunoprecipitation with anti-V5 antibody, bound RNA was purified using Trizol reagent (Invitrogen) and subsequently used in transcript analyses by semiquantitative and real-time RT–PCR.

Antibodies. Mouse anti-V5 (Invitrogen), rat anti-HA (Roche), mouse anti-dFMR 6A15 (Abcam), human anti-P0 (Immunovision), rabbit anti-PER[40], guinea pig anti-TIM[40], rat anti-GE-1[44], rat anti-Tral[44], rabbit anti-dPABP[45] and rabbit anti-eIF4E[46] antibodies were used in our protein analyses.

GST pull-down assay. *In vitro* binding assay was performed as described previously[40] with minor modifications. TYF and deletion mutant proteins were *in vitro* translated in the presence of ^{35}S-methionine using TNT T7 coupled reticulocyte lysate system (Promega).

GST fusion proteins were purified from bacterial cultures using glutathione-Sepharose 4B beads (GE Healthcare) and incubated with ^{35}S-labelled proteins in a binding buffer (20 mM HEPES pH 7.5, 100 mM KCl, 5% glycerol, 1 mM EDTA, 1 mM dithiothreitol, 0.1% Triton X-100, 1 mM phenylmethylsulfonyl fluoride). After the incubation for 1 h at 4 °C, the beads were washed three times in the same buffer. Bound proteins were eluted, resolved by SDS–PAGE, and detected by autoradiography.

Cap pull-down assay. S2 cells in 100-mm dishes were transfected with 1.2 μg of expression vector for TYF–V5 or deletion mutants. Cells were harvested at 48 h after transfection, washed in PBS, and resuspended in a lysis buffer (25 mM Tris-Cl pH 7.5, 150 mM NaCl, 10% glycerol, 1 mM EDTA, 1 mM dithiothreitol, 0.5% Nonidet P-40, 1 mM phenylmethylsulfonyl fluoride, protease inhibitors). Extracts were clarified by centrifugation and incubated with pre-equilibrated m^7-GTP Sepharose 4B (GE Healthcare) for 1.5 h at 4 °C. Where indicated, 0.5 mM m^7-GTP or GTP was added to the lysis buffer. The beads were washed four times with the same buffer. Bound proteins were eluted by boiling in 1× SDS sample buffer, resolved by SDS–PAGE and immunoblotted with antibodies as shown.

Sucrose density gradient fractionation. Sucrose gradient sedimentations were performed as described previously[47,48] with minor modifications. S2 cells were cultured in 100-mm dishes and transfected with 2 μg of Ac/TYF–3×HA using Effectene reagent (Qiagen). At 48 h after transfection, 200 μg ml^{-1} of cycloheximide was added to the media and incubated for a further 10 min. Cells were harvested, washed twice with PBS and lysed in 800 μl of polysome gradient buffer (15 mM Tris-Cl pH 7.5, 300 mM NaCl, 10 mM $MgCl_2$, 0.2 mg ml^{-1} cycloheximide, 50 U ml^{-1} RNasin, 0.1 mg ml^{-1} heparin, 1 mM dithiothreitol, 1 mM phenylmethylsulfonyl fluoride, complete protease inhibitor) containing 0.5% Nonidet P-40. For EDTA treatment, 10 mM $MgCl_2$ in the lysis buffer was replaced by 25 mM EDTA and cycloheximide was omitted. The lysates were incubated for 15 min at 4 °C and centrifuged twice. Clarified lysates were loaded on 10–50% linear sucrose gradient solution. Samples were spun in a SW 41Ti rotor (Beckman) at 36,000 r.p.m. for 2 h. Using tube piercer (Brandel) and FRAC-100, each fraction was collected from the bottom while UV absorbance at 254 nm was monitored continuously with UA-6 detector (ISCO). Proteins in each fraction were precipitated with chloroform/methanol[49] and used for western blotting analyses.

RNA tethering assay. S2 cells on 24-well plates were co-transfected with 5 ng of Ac/FLUC-6×BS (or its derivatives), 25 ng of Ac/RLUC, and 250 ng of Ac/MS2–V5 (or its derivatives). For competition experiments, S2 cells were co-transfected with 5 ng of Ac/5′-UTR-FLUC-3′-UTR-6×BS, 5 ng of Ac/RLUC, 125 ng of Ac/MS2–V5 or Ac/TYF–MS2–V5, and the increasing amount (125 or 375 ng) of Ac/TYF–V5 (or TYF deletion constructs). Cells were harvested at 48 h after transfection and dual luciferase assays were performed according to the manufacturer's instructions (Promega).

Subcellular fractionation. S2 cells were treated with 200 μg ml^{-1} of cycloheximide for 10 min before harvesting at 48 h after transfection. Cell pellets were resuspended in a hypotonic buffer (10 mM HEPES pH 7.9, 1.5 mM $MgCl_2$, 10 mM KCl, 0.5 mM dithiothreitol) on ice for 10 min. Nonidet P-40 were added to a final concentration of 0.5% and incubated for an additional 5 min on ice. Lysates were centrifuged at 5,000 r.p.m. for 5 min. RNA was isolated from supernatant (cytoplasmic fraction) and pellet (nuclear fraction), separately, using Trizol LS and Trizol reagents (Invitrogen), treated with DNase I and DpnI, reverse-transcribed by M-MLV reverse transcriptase (Promega), and quantified by real-time RT–PCR. *Fluc* RNA levels were first normalized to *cyc* RNA levels in each fraction and the ratio of normalized *Fluc* RNA levels in the cytoplasm fraction to the nuclear fraction was compared between MS2- and TYF–MS2-transfected cells.

Sucrose cushion centrifugation. Transfected cells were resuspended in 400 μl of the polysome gradient buffer containing 0.5% Nonidet P-40, homogenized by 20 strokes with a pestle homogenizer and further incubated for 15 min at 4 °C. Lysates were cleared by centrifugation at 12,000 r.p.m. for 5 min at 4 °C, and layered onto a 2 ml of 45% (wt/wt) sucrose cushion in the polysome gradient buffer. Samples were centrifuged in a SW55Ti (Beckman) for 2 h at 50,000 r.p.m. at 4 °C. After the centrifugation, RNA was isolated from sucrose cushion and pellet fractions, separately, using the RNeasy mini kit (Qiagen) and quantified as described earlier. On the basis of the quantification of 18S ribosomal RNA levels, 32 ±5% of total ribosomes were pelleted by their higher density under these conditions. The ratio of normalized *Fluc* RNA levels in pellet fraction to sucrose cushion fraction was compared between MS2- and TYF–MS2-transfected cells.

***In vitro* translation assay.** *In vitro* translation assays using S2 cell extracts were performed as described previously[50,51] with some modifications. S2 cells were harvested and washed three times in PBS. Cell pellets were resuspended and homogenized in 1 volume of hypotonic lysis buffer (10 mM HEPES-KOH pH 7.4, 10 mM KOAc, 0.5 mM $Mg(OAc)_2$, 5 mM dithiothreitol and protease inhibitors). After 10 min incubation on ice, the cell extracts were clarified by centrifugation at 13,000 r.p.m. for 10 min at 4 °C. Supernatants were immediately used in *in vitro* translation reaction or stored at −80 °C. For the template of MS2 reporter RNAs, firefly luciferase cDNA along with *per* 3′ UTR and MS2-binding sites was subcloned into pcDNA3. m^{7}G-capped RNAs were *in vitro* transcribed using mMESSAGE mMACHINE kit (Ambion) and divided into two aliquots. Poly(A) tail (>150 nucleotides) was added to RNA transcripts in one aliquot using Poly(A) Tailing kit (Ambion) according to the manufacturer's instruction. For poly(A)$^-$ reporter RNA, poly(A) polymerase was omitted in a parallel reaction using the other aliquot. All RNAs were further purified using MEGAclear kit (Ambion), quantified, and stored in aliquots at −80 °C until use. m^{7}G-capped and polyadenylated RNA for *Renilla* luciferase was similarly prepared and included as an internal control in *in vitro* translation reactions. Each *in vitro* translation reaction included 5 ng of firefly luciferase RNA containing *per* 3′ UTR and MS2-binding sites, 10 ng of *Renilla* luciferase RNA, 100 ng of bacterially purified GST–MS2 or GST–TYF-C3–MS2, 24 mM HEPES-KOH pH 7.4, 60 mM KOAc, 1.5 mM

$Mg(OAc)_2$, 0.1 mM spermidine, 1.2 mM dithiothreitol, 20 mM creatine phosphate, 60 μM amino acids, 120 μg ml^{-1} creatine kinase, 0.1 mg ml^{-1} yeast tRNA, 4 U RNasin (Promega), and 40% S2 extracts in 12.5 μl reaction. The reaction was incubated for 90 min at 25 °C, stopped by adding 50 μl of 1× Reporter lysis buffer (Promega), and kept on ice. Ten microlitres of the mixture was used for dual luciferase assay as described earlier. Total RNA was purified from the rest of the *in vitro* translation reaction using Triozol and quantified by realtime RT–PCR.

31. Sharma, Y., Cheung, U., Larsen, E. W. & Eberl, D. F. PPTGAL, a convenient *GAL4* P-element vector for testing expression of enhancer fragments in *Drosophila*. *Genesis* **34,** 115–118 (2002).
32. Lykke-Andersen, J., Shu, M. D. & Steitz, J. A. Human Upf proteins target an mRNA for nonsense-mediated decay when bound downstream of a termination codon. *Cell* **103,** 1121–1131 (2000).
33. Kaneko, M. & Hall, J. C. Neuroanatomy of cells expressing clock genes in *Drosophila*: transgenic manipulation of the period and timeless genes to mark the perikarya of circadian pacemaker neurons and their projections. *J. Comp. Neurol.* **422,** 66–94 (2000).
34. Cheng, Y., Gvakharia, B. & Hardin, P. E. Two alternatively spliced transcripts from the *Drosophila* period gene rescue rhythms having different molecular and behavioral characteristics. *Mol. Cell. Biol.* **18,** 6505–6514 (1998).
35. Zhao, J. *et al. Drosophila* clock can generate ectopic circadian clocks. *Cell* **113,** 755–766 (2003).
36. Osterwalder, T., Yoon, K. S., White, B. H. & Keshishian, H. A conditional tissue-specific transgene expression system using inducible *GAL4*. *Proc. Natl Acad. Sci. USA* **98,** 12596–12601 (2001).
37. Groth, A. C., Fish, M., Nusse, R. & Calos, M. P. Construction of transgenic *Drosophila* by using the site-specific integrase from phage phiC31. *Genetics* **166,** 1775–1782 (2004).
38. Markstein, M., Pitsouli, C., Villalta, C., Celniker, S. E. & Perrimon, N. Exploiting position effects and the gypsy retrovirus insulator to engineer precisely expressed transgenes. *Nature Genet.* **40,** 476–483 (2008).
39. Lim, C. *et al.* Clockwork orange encodes a transcriptional repressor important for circadian-clock amplitude in *Drosophila*. *Curr. Biol.* **17,** 1082–1089 (2007).
40. Lim, C. *et al.* Functional role of CREB-binding protein in the circadian clock system of *Drosophila melanogaster*. *Mol. Cell. Biol.* **27,** 4876–4890 (2007).
41. Matsumoto, A. *et al.* A functional genomics strategy reveals clockwork orange as a transcriptional regulator in the *Drosophila* circadian clock. *Genes Dev.* **21,** 1687–1700 (2007).
42. Houl, J. H., Yu, W., Dudek, S. M. & Hardin, P. E. *Drosophila* CLOCK is constitutively expressed in circadian oscillator and non-oscillator cells. *J. Biol. Rhythms* **21,** 93–103 (2006).
43. Picot, M., Cusumano, P., Klarsfeld, A., Ueda, R. & Rouyer, F. Light activates output from evening neurons and inhibits output from morning neurons in the *Drosophila* circadian clock. *PLoS Biol.* **5,** e315 (2007).
44. Eulalio, A., Behm-Ansmant, I., Schweizer, D. & Izaurralde, E. P-body formation is a consequence, not the cause, of RNA-mediated gene silencing. *Mol. Cell. Biol.* **27,** 3970–3981 (2007).
45. Roy, G., Miron, M., Khaleghpour, K., Lasko, P. & Sonenberg, N. The *Drosophila* poly(A) binding protein-interacting protein, dPaip2, is a novel effector of cell growth. *Mol. Cell. Biol.* **24,** 1143–1154 (2004).
46. Nakamura, A., Sato, K. & Hanyu-Nakamura, K. *Drosophila* cup is an eIF4E binding protein that associates with Bruno and regulates *oskar* mRNA translation in oogenesis. *Dev. Cell* **6,** 69–78 (2004).
47. Monzo, K. *et al.* Fragile X mental retardation protein controls trailer hitch expression and cleavage furrow formation in *Drosophila* embryos. *Proc. Natl Acad. Sci. USA* **103,** 18160–18165 (2006).
48. Satterfield, T. F. & Pallanck, L. J. Ataxin-2 and its *Drosophila* homolog, ATX2, physically assemble with polyribosomes. *Hum. Mol. Genet.* **15,** 2523–2532 (2006).
49. Wessel, D. & Flugge, U. I. A method for the quantitative recovery of protein in dilute solution in the presence of detergents and lipids. *Anal. Biochem.* **138,** 141–143 (1984).
50. Thoma, C., Ostareck-Lederer, A. & Hentze, M. W. A poly(A) tail-responsive *in vitro* system for cap- or IRES-driven translation from HeLa cells. *Methods Mol. Biol.* **257,** 171–180 (2004).
51. Castagnetti, S., Hentze, M. W., Ephrussi, A. & Gebauer, F. Control of *oskar* mRNA translation by Bruno in a novel cell-free system from *Drosophila* ovaries. *Development* **127,** 1063–1068 (2000).